# Investigation of nitrogen-related acceptor centers in indium selenide by means of photoluminescence: Determination of the hole effective mass

Ch. Ferrer-Roca, A. Segura, M. V. Andrés, J. Pellicer, and V. Muñoz
*Departamento de Física Aplicada, Universidad de Valencia, Dr. Monliner 50, 46100 Burjassot, Valencia, Spain*
(Received 5 August 1996; revised manuscript 21 October 1996)

In this work we report on steady-state and time-resolved photoluminescence (PL) measurements in nitrogen-doped *p*-type indium selenide in the 33–210-K temperature range. In samples with low nitrogen concentration the photoluminescence spectrum consists of exciton-related peaks and a band-to-acceptor recombination peak (2.1-$\mu$s lifetime) with LO-phonon replica. An ionization energy of 65.5 meV is proposed for the nitrogen-related acceptor. A long-lived (18 $\mu$s) component, which consists of an asymmetric broadband centered around the acceptor peak, has been also detected by means of time-resolved PL. Samples with a higher nitrogen concentration show a PL spectrum that mainly consists of the asymmetric long-lived broadband that can be associated to a complex center. The asymmetric shape of this band is quantitatively accounted for in the framework of the configuration coordinate model for complex centers. Under the assumption that the nitrogen-related acceptor is shallow, the Gerlach-Pollman theory allows an estimate of the hole's effective masses, yielding $m^*_{h\perp}=(0.73\pm0.09)m_0$ and $m^*_{h\|}=(0.17\pm0.03)m_0$.
[S0163-1829(97)03811-3]

## I. INTRODUCTION

Bridgman grown crystals of the III-VI layered semiconductor indium selenide (InSe) are *n* type when no acceptor impurities are added. Such *n*-type conductivity has been shown to be due to a shallow native donor, with an ionization energy of 17.4 meV, as determined from far-infrared absorption.[1,2] The existence of such a donor has allowed an accurate determination of the electron effective-mass tensor through cyclotron resonance experiments.[3] For shallow acceptors, no good estimate of the hole effective masses exists to our knowledge. Any advance in this direction depends on the possibility of finding a suitable acceptor impurity, creating shallow acceptor levels with a low degree of compensation. Impurities from groups I to V are known[4] to create acceptor levels in InSe, but the resulting material always presents a high degree of compensation and relatively low conductivity. Photoluminescence spectra in those crystals are mainly dominated by broadbands that have been interpreted as arising from complex centers formed by the substitutional acceptor impurity associated to native or self-compensating donors.[5–11] From the analysis of those photoluminescence (PL) spectra, acceptor-level ionization energies ranging from 50 to 90 meV have been proposed.[5,6]

Nitrogen has been shown to behave as an acceptor in gallium selenide[12] In the present paper nitrogen-doped *p*-type InSe is studied. Results from continuous, time-resolved PL spectra, and PL time decay measurements at different temperatures are presented in Sec. III. In view of the results, the origin of the PL peaks is discussed in Sec. IV and a calculation based on an anisotropic hydrogenic model yields an estimate of the hole effective masses.

## II. EXPERIMENTAL SETUP

The *p*-type InSe crystals used in this study have been grown by the Bridgman-Stockbarger method from a non-stoichiometric polycrystalline melt ($In_{1.05}$ $Se_{0.95}$) to which different amounts of indium nitride were added. Ingots used here have been grown from melts in which the initial concentrations of nitrogen were 0.5 and 1 at. %, to which we will refer as ingots $I_{0.5}$ and $I_1$, respectively. The strong segregation coefficient of impurities in InSe (Refs. 4 and 13) makes the actual concentration in the ingot much lower. Most of the impurities are rejected to the ingot end, together with excess indium, during the Bridgman growth. From Hall effect measurements, the whole concentration at room temperature is of the order of $10^{14}$ and $10^{15}$ $cm^{-3}$ in $I_{0.5}$ and $I_1$, respectively. This does not correspond to the actual acceptor concentration due to the presence of compensating native donors. Both donor and acceptor concentrations can be estimated from the temperature dependence of the hole concentration and mobility, according to the model described in Ref. 5. The acceptor concentrations are of the order $10^{16}$ and $10^{17}$ $cm^{-3}$ for ingots $I_{0.5}$ and $I_1$, respectively.

In order to investigate the possible inhomogeneous distribution of impurities, samples from the InSe monocrystal point *P* (beginning of the growth) and the monocrystal end *E* (last stage of the InSe growth) were studied. We will refer to those samples as $P_{0.5}$, $P_1$, $E_{0.5}$, and $E_1$, where the subscripts indicate the initial concentration percentage. Samples were prepared by cleaving from both ingots with a razor blade and had typical dimensions of $3\times3$ mm in size and around 50 $\mu$m in thickness.

PL low-temperature experiments were carried out in a He closed cycle Leybold-Heraeus cryogenic system. The excitation source was a 100-mW tunable $Ar^+$ laser at 488 nm. The beam was focused on the sample surface and the maximum photon flux was of the order of $5\times10^{20}$ photons $s^{-1}$ $cm^{-2}$. The laser beam was modulated at 1000 Hz with a 80-MHz Bragg cell driven by a 1-kHz square wave having a decay time of 20 ns. The rise and fall time of the laser pulses was lower than 0.2 $\mu$s, a value basically determined by the time

 

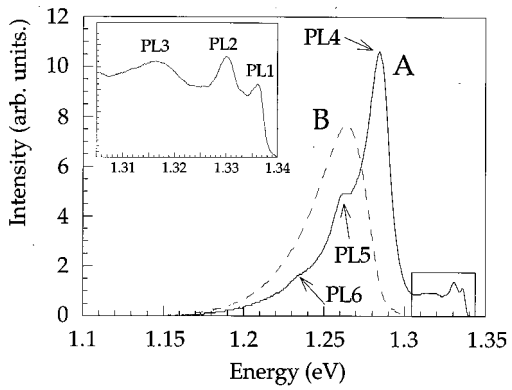


FIG. 1. Representative N-InSe spectra: type *A* spectrum (solid line) with the peak labels from PL1 to PL6; type *B* spectrum (discontinuous line), consisting of a broad band, characteristic of the upper part of the high dopant concentration ingot.

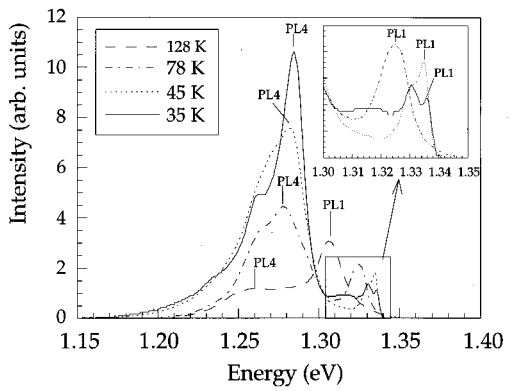


FIG. 2. Type *A* spectrum evolution at four representative temperatures. The smaller graph shows the higher energy part in greater detail.

response of the Bragg cell. The PL light was analyzed with a TRH-1000 Jobin-Yvon monochromator with 1-m focal length and wavelength dispersion of 16 Å/mm at the focal plane. The slit width was 1 mm for steady-state measurements and 3 mm for time-resolved and time-decay measurements. The detector was a Si photodiode with a 125-MHz bandwidth amplifier.

To record steady-state PL spectra, the detector signal was synchronously measured with a lock-in amplifier and subsequently acquired. For time-decay measurements, the square wave that drives the Bragg cell was used as an external trigger for a Hewlett-Packard 400-MHz digital oscilloscope where the PL decay was visualized and subsequently acquired, after having passed through a 50-MHz dc-coupled amplifier and filtered with a 10-MHz low pass filter for noise reduction. Further signal-to-noise improvement was achieved by averaging 2048 sweeps. Time-resolved spectroscopy was carried out using a boxcar integrator and a 100-ns gate, which allowed for the PL acquisition at different delay times.

## III. RESULTS

Figure 1 shows two typical PL spectra at low temperature (35 K). Type *A* spectrum (characteristic of samples $P_{0.5}$, $E_{0.5}$, and $P_1$) consists of some low-intensity, high-energy peaks, labeled PL1, PL2, and PL3, at energies 1.336, 1.330, and 1.316 eV, respectively (they can be seen in detail, with a higher resolution, on the upper left), and a higher-intensity peak (labeled PL4) at 1.285 eV, which slowly decreases for decreasing energies, showing two prominences (labeled PL5 and PL6) at approximately 1.26 and 1.236 eV. Type *B* spectrum (observed in samples $E_1$) presents instead an asymmetric broad band with its maximum around 1.265 eV. Samples $E_1$ can also exhibit a mixture of *A* and *B* spectra.

Figure 2 shows PL spectrum *A* at four different temperatures. In the high-energy region, peak PL3 quickly decreases between 35 and 45 K. Peak PL2 also decreases, although at a lower rate, and is no longer observable at 78 K. Only peak PL1 remains observable in the whole temperature range. Its intensity slowly increases up to 128 K, and then starts a decreasing tendency. In the lower-energy range, structures PL5 and PL6 become less pronounced above 45 K but remain still observable as shoulders of the PL4 peak up to 78 K. Peaks PL1 and PL4 shift to lower energies with increasing temperature, as shown in Fig. 3(a). The temperature shift of the peak in type *B* spectra is shown in Fig. 3(b). It must be pointed out that above 100 K all peaks shift to lower energies with a temperature coefficient of $-4$ meV/K, the same as the InSe band gap.[14] The thermal quenching activation energies for the type *A* (PL4) and type *B* spectra are 43 and 88 meV, respectively, as obtained from the Arrhenius plot of the PL intensity.

Time decay measurements have been performed at different temperatures and photon energies. Samples with the type *B* PL spectrum exhibit a single component with a time decay of $16.26 \pm 0.13$ $\mu$s at 33 K. Samples with the type *A* spectrum exhibit time decays with several components as shown

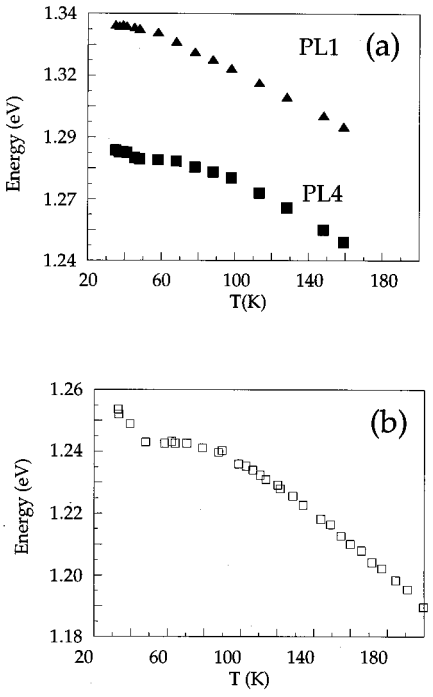


FIG. 3. Energy shift vs temperature of (a) PL1 and PL4 in type *A* spectrum, (b) broad band peak in type *B* spectrum.

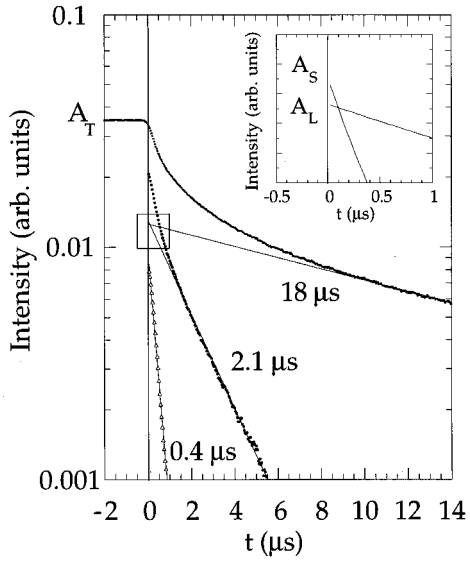


FIG. 4. Logarithmic plot of the PL4 (type *A* spectrum) time decay signal at 35 K, having an amplitude $A_T$ at time zero. A fit of the linear part yields an exponential with a time decay of 18 $\mu$s. The amplitude of that component at time zero is $A_L$ (see the smaller graph). The subtraction of that fit to the original signal yields another component with a time decay of 2.1 $\mu$s, with an amplitude $A_S$ at time zero. The remaining signal linear fit has a time decay of 0.4 $\mu$s, which is of the same order of the laser modulating decay time.

in the logarithmic plot of Fig. 4. A fit of the linear part and subsequent subtraction from the signal leads to the isolation of three different lifetimes, which are $18.0\pm0.1$, $2.14\pm0.01$, and $0.38\pm0.01$ $\mu$s at 35 K. The intersect of each linear fit with the time origin gives the amplitude of that component at time zero. Figure 5 shows the Arrhenius plot of the first two decay times and their respective amplitudes at time zero. The correlation between time decay and amplitude is evident. A

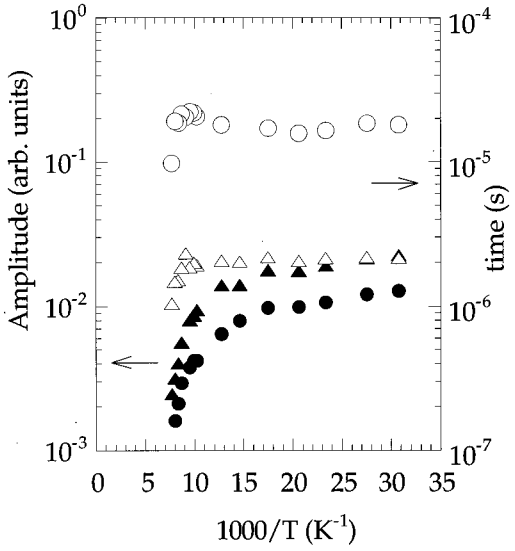


FIG. 5. Amplitude (left scale: ●, long-lived component; ▲, short-lived component) and time decay of PL4 (right scale: ○, long-lived component; △, short-lived component) vs the inverse of temperature.

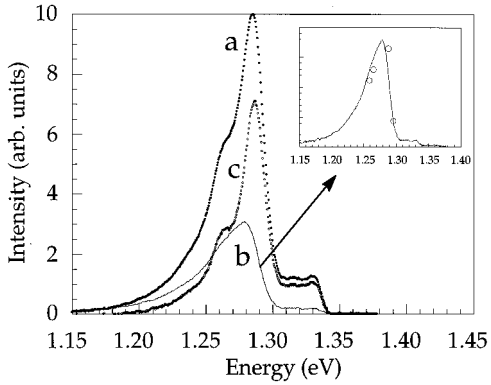


FIG. 6. Long-lived and short-lived contributions to type *A* spectrum: (a) overall spectrum, (b) long-lived component spectrum, (c) short-lived component spectrum, obtained by subtracting (b) from (a). The smaller graph on the upper right represents the long-lived component (b) and four points determined by time decay measurements.

linear fit of the linearly decreasing amplitude portion has yielded the following approximate activation energies: 70–80 meV for the long-lived component and 56 meV for the short-lived one.

Time-resolved spectra at time delays longer than 15 $\mu$s contain exclusively the long-lived component. Its contribution to the steady-state PL spectrum can be obtained by simply multiplying by a factor. Such a factor is calculated in order to give the same amplitude obtained from time-decay measurements at a given photon energy, in our case $E=1.285$ eV (Fig. 6). As verification, this procedure has been carried out at different energies around the peak PL4 (1.259, 1.265, and 1.296 eV) and similar results have been obtained (inset of Fig. 6).

After having subtracted the long-lived component to the type *A* spectrum, the prominences labeled PL5 and PL6 in the low-energy tail of peak PL4 become more evident. Their energies (1.285, 1.260, and 1.236) are equidistant within the experimental error. The whole suggests that this part of the spectrum is a superposition of several components. Figure 7 shows a decomposition of the experimental spectrum in four Gaussians through a fitting procedure carried out in steps. In each step a Gaussian was fitted to the highest-energy and -intensity peak, and then subsequently subtracted from the

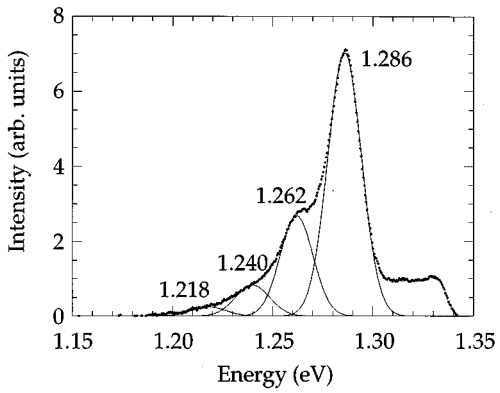


FIG. 7. Type *A* spectrum. A Gaussian fit applied successively to each peak allows for the isolation of PL4, PL5, and PL6.

raw spectrum. In that way peak PL5 (1.262 eV) is clearly evidenced and, following the same procedure, also peak PL6 (1.24 eV) and a new emerging peak, which was not visible in the PL spectrum (1.218 eV), have been isolated.

## IV. DISCUSSION

Let us first discuss the results regarding samples with spectra of the *A* type. From its energy position and temperature shift, we assume that the peak PL1 can be identified as the free exciton radiative recombination peak.[5,15] From its energy and thermal quenching behavior, peaks PL2 and PL3 can be associated to the radiative recombination of bound excitons.[5,15,16] The shortest time decay PL4 component (0.38 $\mu$s), of the same order as the resolution time of our modulation and detection system, can be a contribution of those peaks, since the time decay measurements have been carried out with a lower-energy resolution.

Let us now concentrate on peak PL4 and its tail, which at low temperature can be divided into four equidistant peaks. Peaks with similar structure have been found in GaAs doped with different acceptor impurities such as Cu, Mn, Cd, and Zn, and identified as band-to-acceptor radiative recombination, with replica due to LO-phonon coupling.[17] In polar crystals (ZnS, CdS, and ZnO) Hopfield[18] observed also the occurrence of a series of equally spaced narrow emission lines, decreasing in intensity at longer wavelengths, and suggested the same explanation. According to Hopfield, the separation between the emission lines corresponds to the energy of a longitudinal optical phonon. In our case, the energy distance between peaks is $24\pm2$ meV, very close to the LO optical phonon energies reported for InSe which are 24.6 meV (LO parallel to the *c* axis) and 26.2 meV (LO perpendicular to the *c* axis).[19]

Hence, assuming that peak PL4 is the (zero phonon) band-to-acceptor recombination peak, with a lifetime of 2.1 $\mu$s, we can derive the acceptor binding energy $\Delta E_A$ from its energy and that of the free exciton peak: $\Delta E_A E_{\mathrm{PL1}} - E_{\mathrm{PL4}} + \Delta E_{\mathrm{ex}}$. The exciton binding energy is[14] $\Delta E_{\mathrm{ex}} = E_{\mathrm{gap}} - E_{\mathrm{ex}} = 14.5$ meV. From the spectrum $E_{\mathrm{PL4}} = 1.285$ eV and $E_{\mathrm{PL1}} = 1.336$ eV (both at 35 K), then the acceptor binding energy at 35 K would be $\Delta E_A = 65.5$ meV. This value is consistent with the calculated quenching activation energy and with the predictions mentioned in the Introduction.[5,6]

According to Hopfield,[18] the mean number of emitted phonons, which corresponds to the intensity ratio between the one-phonon peak and the zero-phonon peak, is given by

$$\langle N\rangle = \frac{e^2}{a}\frac{1}{(\hbar\omega)_{\mathrm{LO}}}\frac{1}{\sqrt{2\pi}}\left(\frac{1}{\epsilon_\infty}-\frac{1}{\epsilon_0}\right), \tag{1}$$

where $a$ is the hole effective Bohr radius in the acceptor level ($a = e^2/2\epsilon_0\Delta E_A$, assuming an impurity hydrogenic model for the acceptor), and $h\omega_{\mathrm{LO}}$ the phonon energy. The low-frequency dielectric constants in InSe can be obtained from the values given in the literature for their product and ratio[2]: $\epsilon_{0\perp}\epsilon_{0\parallel} = (80.7\pm1.3)\epsilon_0^2$ and $\epsilon_{0\perp}/\epsilon_{0\parallel} = (1.31\pm0.15)$, we obtained $\epsilon_{0\perp} = (10.3\pm0.6)\epsilon_0$ and $\epsilon_{0\parallel} = (7.9\pm0.5)\epsilon_0$, where $\epsilon_0$ is the vacuum dielectric constant. The high-frequency values can be calculated from the Lyddane-Sachs-Teller relation $\epsilon_\infty = (\omega_{\mathrm{LO}}/\omega_{\mathrm{TO}})^{-2}\epsilon_0$. The reported phonon transverse optic wave-number values are[19] $\kappa_\perp = 180\ \mathrm{cm}^{-1}$ and $\kappa_\parallel = 191\mathrm{cm}^{-1}$, hence $\epsilon_{\infty\perp} = 7.5\epsilon_0$ and $\epsilon_{\infty\parallel} = 7.3\epsilon_0$.

Because InSe is an anisotropic semiconductor, Eq. (1) leads to two different phonon mean numbers, $\langle N\rangle_\perp = 0.64$ and $\langle N\rangle_\parallel = 0.17$, whose average would be $(2\langle N\rangle_\perp + \langle N\rangle_\parallel)/3 = 0.48$, very close to the experimental ratio from peaks PL4 to PL5, which yields 0.38, suggesting that our assumption of considering peak PL4 and its tail as an acceptor peak with its phonon replica is correct.

The behavior of the acceptor and exciton energy shift with temperature [Fig. 3(a)] contributes to the confirmation of our hypothesis, as both show the same decreasing tendency by keeping their distance approximately constant.

Once the acceptor ionization energy $\Delta E_A$ has been determined, the hole effective-mass tensor can be estimated on the assumption that it corresponds to a hydrogenic anisotropic acceptor. We will use the energy expressions calculated by Gerlach and Pollmann[20] for anisotropic hydrogenic impurity levels:

$$E_{(nl)m}(\alpha) = -\frac{R}{n^2}Z^2_{1|m|}(\alpha), \tag{2}$$

where $\alpha = 1 - A$ is the anisotropy parameter, $A = m^*_\perp\epsilon_{0\perp}/m^*_\parallel\epsilon_{0\parallel}$ is the anisotropy ratio, $Z(\alpha)$ the effective charge, and $R = \beta m^*_\perp$ the Rydberg energy with $\beta = 13.6\epsilon_0{}^2/\epsilon_{0\perp}\epsilon_{0\parallel}$. Assuming that we know the acceptor and exciton ionization energies (binding energy at the $n=1$ state), we can get two energy equations in which only the effective charge $Z_{00}(\alpha)$ is involved:

$$\Delta E_A = R_h Z^2_{00}(\alpha_h) \quad \text{(a)},$$

$$\Delta E_{\mathrm{ex}} = R_{\mathrm{ex}} Z^2_{00}(\alpha_{\mathrm{ex}}) \quad \text{(b)}, \tag{3}$$

where

$$Z_{00}(\alpha) = \frac{1}{\sqrt{|\alpha|}}\,\mathrm{arcsinh}\sqrt{|\alpha|}, \quad \alpha < 0 \tag{4}$$

and $R_h$, $\alpha_h$, and $R_{\mathrm{ex}}$, $\alpha_{\mathrm{ex}}$ refer, respectively, to the hole and exciton Rydberg and anisotropy parameters.

We can obtain, from Eq. (3a), an expression for the perpendicular hole effective mass:

$$m^*_{h\perp} = -\frac{\Delta E_{\alpha h}}{\beta C^2}, \quad C = \mathrm{arcsinh}(\sqrt{|\alpha_h|}), \tag{5}$$

which, introduced in Eq. (3b), gives the following equality:

$$\sinh\left[\left(\frac{\Delta E_{\mathrm{ex}}}{\Delta E_A}C^2 + \frac{\Delta E_{\mathrm{ex}}(_e-1)}{R_e}\right)^{1/2}\right] = \left(|\alpha_h|\frac{R_e C^2 + \Delta E_A(A_e-1)}{R_e C^2 + \Delta E_A}|\alpha_h|\right)^{1/2}, \tag{6}$$

where $A_e$ and $R_e$ are the electron anisotropy ratio and the electron Rydberg energy, respectively. These values are well determined in InSe ($A_e = 2.28\pm0.02$ and $R_e = 191.8\pm0.15$) from the energy structure of donor levels.[2] We can then get a solution (the holes anisotropy ratio) from the crossing of

both sides of Eq. (6). Thus, by taking into account Eq. (5), we can determine both perpendicular and parallel holes effective masses.

In order to do that, we must take into account the error that affects both $R_e$ and $A_e$ (or, equivalently, the error that affects the dielectric constants $\epsilon_{0\perp}$ and $\epsilon_{0\parallel}$) and the electron effective masses that are reported in the literature[3] [$m^*_{e\perp}=(0.141\pm0.002)m_0$ and $m^*_{e\parallel}=(0.081\pm0.009)m_0$].

By combining different perpendicular and parallel dielectric constants in the range [10.1, 9.7] and [8.2, 7.3], respectively (both ranges are included in the respective error intervals) and introducing the experimental acceptor binding energy $\Delta E_A=65.5$ meV in Eq. (6), different crossing points are obtained corresponding to anisotropy ratio $A_h$ values in the interval [9.3, 2.81]. Consequently, perpendicular and parallel hole effective masses are in the range [0.91, 0.56] and [0.24, 0.13], respectively. The hole effective masses mean values and standard deviations obtained by averaging over all the crossing points yield $m^*_{h\perp}=(0.73\pm0.09)m_0$ and $m^*_{h\parallel}=(0.17\pm0.03)m_0$.

Previously and from a similar basis, Segura *et al.*[5] had proposed $m^*_h\approx0.6m_0$. Given the similarity between the valence-band structure of InSe and GaSe (that are formed in both compounds from Se $p_z$ states) it would be reasonable to expect similar hole effective mass values in both compounds. The values proposed for GaSe by Ottaviani *et al.*[21] ($m^*_{h\perp}=0.8m_0$ and $m_{h\parallel}0.8m_0$ and $m^*_{h\parallel}=0.2m_0$) and Piccioli[22] ($m^*_{h\perp}=0.71m_0$ and $m^*_{h\parallel}=0.17m_0$) are indeed very close to those here estimated for InSe.

On the other hand, the density-of-states effective mass in the valence band would be $m^*_{vd}=(m^{*2}_{h\perp}m^*_{h\parallel})^{1/3}=0.45m_0$, which is well below the values found in the literature from combined Hall effect and thermopower measurements ($m^*_{hd}\approx1.5m_0$).[23] It must be outlined that the estimation of effective masses from transport measurements are very much dependent on the hole scattering mechanisms, which are not well known due to the overcompensated character of $p$-InSe samples.

The PL4 measured lifetime is also consistent with its identification as band to acceptor recombination. According to Barry and Williams[24] this lifetime is given by

$$\tau^{-1}_{(T\to0)}=p_A\frac{2^5h^2}{\pi{m_0}^2c}\left(\frac{m_A}{m_0}\right)\left(\frac{a_A}{a_0}\right)\left(\frac{E_{cv}}{\Delta E_A}\right)\left(\frac{h\upsilon}{m_0c^2}\right)n, \quad (7)$$

with $p_A$ the acceptor level concentration, $m_A$, $a_A$, and $\Delta E_A$ the acceptor effective mass, Bohr radius, and energy, respectively, $E_{cv}$ the transition matrix element, $h\upsilon$ the transition energy, and $n$ the refractive index. By taking $E_{cv}=0.6$ eV,[14] $m_A=m^*_{vd}=0.45m_0$ and $\Delta E_A=65.5$ meV, $h\upsilon=1.28$ eV, and $\tau=2.1$ $\mu$s, Eq. (7) yields an acceptor concentration of $2\times10^{16}$ cm$^{-3}$, a value that is coherent with those estimated from the temperature dependence of hole concentration and mobility.

Let us discuss the origin of type $B$ spectra. First of all it must be pointed out that the broadband spectrum that appears for longer times in type $A$ spectra has the same form and a decay time of the same order as the one characteristic of spectrum $B$, suggesting a common origin in both cases. On the other hand, its form and temperature dependence are very similar to those of PL spectra of Cd-doped InSe, attributed to self-activated luminescence in a complex center.[6] In our case, the same indium atom in interstitial position proposed there would be a good candidate for the donor whereas nitrogen would substitute the selenium atom, acting as an acceptor. This hypothesis could justify the fact that the broadband spectrum (type $B$) appears predominantly in samples $E_1$. This can be explained through the fact that nitrogen was introduced as InN into the polycrystalline melt. A large part of the InN can decompose, liberating the nitrogen as $N_2$ molecules and giving rise to an indium excess. Even if most In atoms are rejected to the end of the ingot during the crystal growth (InSe can only be grown from melts with indium excess), a part of them can remain in interstitial positions and associate to substitutional acceptors, giving rise to the complex centers.

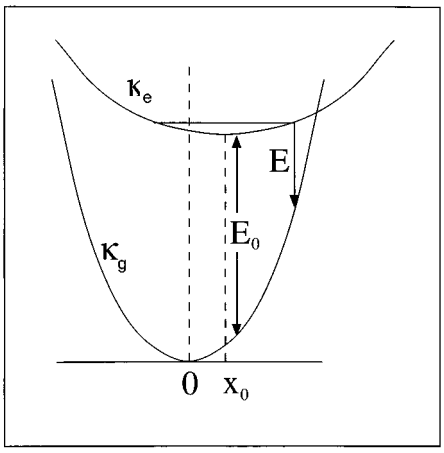


FIG. 8. CC diagram for the complex center.

In the framework of the configurational coordinate (CC) model for complex centers, asymmetric Gaussian bands correspond to complex centers in which the minima of the ground and excited state occur for very close values of the configuration coordinate $x$. This happens when the donor, the acceptor, or both have a shallow character; i.e., their wave functions extend over several unit cells.[24] In that case, transitions between both states do not lead to strong charge rearrangement and lattice relaxation. In order to account for the shape of type $B$ spectra, let us describe the ground and excited state of the centers as two parabolas:[25]

$$E_g(x)=\tfrac{1}{2}\kappa_g x^2, \quad E_e(x)=\tfrac{1}{2}\kappa_e(x-x_0)^2+E_{0e}, \quad (8)$$

where $\kappa_g$ and $\kappa_e$ are the ground and excited level elastic constants, respectively (see Fig. 8). Assuming a Maxwell-Boltzmann distribution of electrons in the excited state, the semiclassical approximation[26] leads straightforwardly to the following spectral shape:

$$I(E)=\frac{A}{\sqrt{1-B(E-E_0)}}\exp\left(-\frac{[1-\sqrt{1-B(E-E_0)}]^2}{2\sigma^2}\right), \quad (9)$$

with

$$B=\frac{\kappa_e-\kappa_g}{\kappa_g^2x_0^2}, \quad \sigma=\left(\frac{Bk_BT_{\rm eff}(\kappa_e-\kappa_g)}{\kappa_e}\right)^{1/2},$$

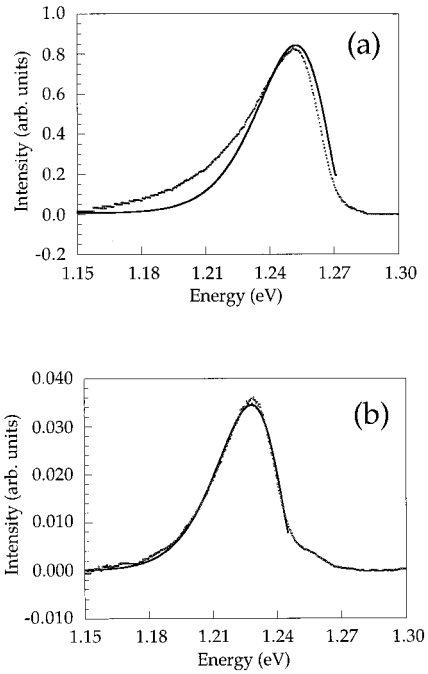


FIG. 9. (a) Type $B$ spectrum at 33 K (points) and theoretical fit (solid line), which yields the following parameter values: $A=0.402$, $B=40.4$, $\sigma=0.336$, $E_0=1.245$ eV. (b) Same at (a) at 134 K, in this case: $A=0.0207$, $B=42.9$, $\sigma=0.312$, $E_0=1.2173$ eV.

$$T_{\text{eff}}=\frac{h\upsilon_e}{2k_B}\coth\left(\frac{h\upsilon_e}{2k_BT}\right),$$

where $A$ is an arbitrary factor.

Figures 9(a) and 9(b) show the fit of Eq. (9) to the experimental type $B$ spectral points at two different temperatures, obtained by leaving $A$, $B$, $E_0$, and $\sigma$ as free parameters. The agreement of the CC model for complex centers with the experimental data is excellent at 134 K; it becomes worse at 33 K owing to the losss of validity of the semiclassical approximation at low temperatures. A broadening of the spectrum with temperature is not experimentally observed, suggesting that the energy of the phonon interacting with the excited level is very high.

## V. SUMMARY

*N*-doped InSe samples have been investigated. PL measurements have shown the presence of two types of spectra: *A* (consisting of three high-energy, low-intensity peaks and a high-intensity peak at 1.285 eV that shows a decaying ''tail'' with some prominences) and *B* (broadband, which presents no details in its structure, appearing only in high dopant concentration samples and belonging to the upper part of the ingot). Time decay measurements yield two lifetimes, 18 and 2.1 $\mu$s, at the 1.285-eV peak of the type *A* spectrum and one of 16.3 $\mu$s for the type *B* spectrum. Time-resolved photoluminescence allowed for the isolation of the long-lived spectrum component, which consists of an asymmetric broad band similar to type *B* spectrum.

The peak at 1.285 eV in the type *A* spectrum has been associated to the recombination with a single acceptor center, leading to an acceptor binding energy of 65.5 meV at 35 K. The observed prominences have been attributed to a phononic replica of the acceptor peak, given that their energy distances coincide with LO optic phonon energies in InSe and the mean phonon number calculated value is in agreement with the experimental one. The higher-energy peaks are related to free and bound exciton recombinations. The agreement of experimental points with a fit of the type *B* spectrum, assuming a spectral shape based on a CC model for complex centers, has led to the identification of such a broad band as a recombination in a complex center. Also the long-lived component in the type *A* spectrum seems to have the same origin, as its shape and time decay suggest. A good candidate as a donor could be the indium atom on the interstitial position, as proposed in previous papers and in accordance with the fact that the type *B* spectrum is predominant in those samples in which the indium concentration is supposed to be higher.

A calculation based on the Guerlach and Pollman hydrogenic model has allowed for an estimate of the holes effective masses, yielding $m^*_{h\perp}=(0.73\pm0.09)m_0$ and $m^*_{h\parallel}=(0.17\pm0.03)m_0$.

## ACKNOWLEDGMENTS

Financial support from Spanish Government CICYT (Project No. MAT95-0391 and associated Grant No. PN95 24351846) and from the Generalitat Valenciana (project GV2205/94) is acknowledged.

[1] E. Kress-Rogers, G. F. Hopper, R. J. Nicholas, W. Hayes, K. Wünstel, and A. Chevy, Appl. Phys. A **31**, 139 (1983).
[2] J. Martinez-Pastor, A. Segura, C. Julien, and A. Chevy, Phys. Rev. B **46**, 4607 (1992).
[3] E. Kress-Rogers, R. J. Nicholas, J. C. Portal, and A. Chevy, Solid State Commun. **44**, 379 (1982).
[4] A. Chevy, These d'Etat, Université de Paris VI, 1982.
[5] A. Segura, M. C. Martínez-Tomás, B. Marí, A. Casanovas, and A. Chevy, Appl. Phys. A **44**, 249 (1987).
[6] M. C. Martínez-Tomás, V. Muñoz, M. V. Andrés, A. Segura, and A. Chevy, Z. Phys. B **91**, 25 (1993).
[7] T. Ikari, S. Shigetomi, Y. Koga, and S. Shigetomi, Phys. Status Solidi B **103**, k81 (1981).
[8] T. Ikari, S. Shigetomi, Y. Koga, and S. Shigetomi, Jpn. J. Appl. Phys. **20**, L343 (1981).
[9] P. Houdy, Thèse de Troisième Cycle, Université de Paris VI 1982).
[10] D. V. Korbutyak, L. A. Demchina, V. G. Litovchenko, and Z. D. Kovalyuk, Poluprovodn. Fiz. Tekh. **17**, 814 (1983) [Sov. Phys. Semicond. **17**, 508 (1983)].
[11] S. Shigetomi, H. Ohkubo, and T. Ikari, J. Phys. Chem. Solids **51**, 91 (1990).
[12] J. F. Sánchez-Royo, A. Segura, A. Chevy, and L. Roa. J. Appl. Phys. **79** (1996).
[13] A. Chevy, J. Appl. Phys. **56**, 978 (1984).
[14] J. Camassel, P. Merte, H. Mathieu, and A. Chevy, Phys. Rev. B **17**, 4718 (1978).
[15] J. Riera, A. Segura, and A. Chevy, Phys. Status Solidi A **142**, 265 (1994).
[16] M. O. Godzaev and B. E. Sernelius, Phys. Rev. B **33**, 8568 (1986).

[17] E. W. Williams, Brit. J. Appl. Phys. **18**, 253 (1967).
[18] J. J. Hopfield. J. Phys. Chem. Solids **10**, 110 (1959).
[19] *Physics of Non-tetrahedrally Bonded Binary Compounds II*, edited by O. Madelung, M. Schulz, and H. Weiss, Landolt-Bornstein, New Series, Group III, Vol. 17, Pt. f (Springer-Verlag, Berlin, 1983).
[20] B. Guerlach and J. Pollmann, Phys. Status Solidi B **67**, 93 (1975).
[21] G. Ottaviani, C. Canali, F. Nava, Ph. Schmid, E. Mooser, R. Minser, and I. Zschokke, Solid State Commun **14**, 933 (1974).
[22] Norbert Piccioli, Thèse de Doctorat d'état, Université Pierre et Marie Curie, 1987.
[23] A. Segura, C. Martínez-Tomás, A, Casanovas, A. Cantarero, J. Martínez-Pastor, and A. Chevy, Appl. Phys. A **48**, 45 (1989).
[24] H. Barry and E.W. Williams, *Semiconductors and Semimetals* Vol. 8 (Academic, New York, 1972).
[25] C. C. Khick and J. H. Schulman, *Solid State Physics* (Academic, New York, 1957), Vol. 5.
[26] F. E. Williams and M. H. Hebb, Phys. Rev. **84**, 1181 (1951).